THE JOURNAL OF BIOLOGICAL CHEMISTRY
Vol. 278, No. 47, Issue of November 21, pp. 47129–47135, 2003
Printed in U.S.A.

Characterization of Perceived Hyperoxia in Isolated Primary Cardiac Fibroblasts and in the Reoxygenated Heart*[S]

Received for publication, August 6, 2003
Published, JBC Papers in Press, September 2, 2003, DOI 10.1074/jbc.M308703200

Sashwati Roy, Savita Khanna, William A. Wallace, Jani Lappalainen, Cameron Rink, Arturo J. Cardounel‡, Jay L. Zweier‡, and Chandan K. Sen§

From the Laboratory of Molecular Medicine, Departments of Surgery and ‡Internal Medicine, Davis Heart and Lung Research Institute, The Ohio State University Medical Center, Columbus, Ohio 43210

Under normoxic conditions, pO_2 ranges from 90 to <3 torr in mammalian organs with the heart at ~35 torr (5%) and arterial blood at ~100 torr. Thus, "normoxia" for cells is an adjustable variable. In response to chronic moderate hypoxia, cells adjust their normoxia set point such that reoxygenation-dependent relative elevation of pO_2 results in perceived hyperoxia. We hypothesized that O_2, even in marginal relative excess of the pO_2 to which cells are adjusted, results in the activation of specific O_2-sensitive signal transduction pathways that alter cellular phenotype and function. Thus, reperfusion causes damage to the tissue at the focus of ischemia while triggering remodeling in the peri-infarct region by means of perceived hyperoxia. We reported first evidence demonstrating that perceived hyperoxia triggers the differentiation of cardiac fibroblasts (CF) to myofibroblasts by a p21-dependent mechanism (Roy, S., Khanna, S., Bickerstaff, A. A., Subramanian, S. V., Atalay, M., Bierl, M., Pendyala, S., Levy, D., Sharma, N., Venojarvi, M., Strauch, A., Orosz, C. G., and Sen, C. K. (2003) *Circ. Res.* 92, 264–271). Here, we sought to characterize the genomic response to perceived hyperoxia in CF using GeneChips™. Candidate genes were identified, confirmed and clustered. Cell cycle- and differentiation-associated genes represented a key target of perceived hyperoxia. Bioinformatics-assisted pathway reconstruction revealed the specific signaling processes that were sensitive to perceived hyperoxia. To test the significance of our *in vitro* findings, a survival model of rat heart focal ischemia-reperfusion (I-R) was investigated. A significant induction in p21 mRNA expression was observed in I-R tissue. The current results provide a comprehensive molecular definition of perceived hyperoxia in cultured CF. Furthermore, the first evidence demonstrating activation of perceived hyperoxia sensitive genes in the cardiac I-R tissue is presented.

Cellular oxygen (O_2) concentrations are maintained within a narrow "normoxic" range to circumvent the risk of oxidative damage from excess O_2 (hyperoxia) and of metabolic demise from insufficient O_2 (hypoxia) (1). pO_2 ranges from 90 to below 3 torr in mammalian organs under normoxic conditions with arterial pO_2 of about 100 torr or ~14% O_2 (2). Thus, "normoxia" for cells is an adjustable variable that is dependent on the specific localization of the cell in organs and functional status of the specific tissue. O_2 sensing is required to adjust to physiological or pathophysiological variations in pO_2. Current work in this field is almost exclusively focused on the study of hypoxia. Reoxygenation, on the other hand, has been mostly investigated in the context of oxidative injury.

Ischemia in the heart results in a hypoxic area containing a central focus of near-zero O_2 pressure bordered by tissue with diminished but nonzero O_2 pressures. These border zones extend for several millimeters from the hypoxic core, with the O_2 pressures progressively increasing from the focus to the normoxic region (3). Moderate hypoxia is associated with a 30–60% decrease (~1–3% O_2) in pO_2 (4). During chronic hypoxia in the heart, cells adjust their normoxic set point such that the return to normoxic pO_2 after chronic hypoxia is perceived as relative hyperoxia. Cardiac fibroblasts (CF)[1] are mainly responsible for the synthesis of major extracellular matrix in the myocardium including fibrillar collagen types I and III and fibronectin. More than 90% of the interstitial cells of the myocardium are fibroblasts (5), which actively cross-talk with myocytes to determine the quantity and quality of extracellular matrix. We have recently observed that CF, isolated from adult murine ventricle, cultured in 10 or 21% O_2 (high O_2, *relative* to the pO_2 to which cells are adjusted *in vivo*), compared with 3% O_2 (mildly hypoxic), exhibit reversible growth inhibition and a phenotype indicative of differentiation. We reported that marginal relative elevation in pO_2, compared with pO_2 to which cells are adjusted during chronic moderate hypoxia, serve as a signal to trigger CF differentiation and tissue remodeling. $p21^{Waf1/Cip1/Sdi1}$ was identified as a key mediator of signaling triggered by perceived hyperoxia (6). Thus, while acute insult during reperfusion may be lethal to cells localized at the focus of insult, sudden relative elevation of O_2 tension in the surrounding peri-infarct ischemic tissue is expected to trigger phenotypic changes in the surviving fibroblasts that may be associated with tissue remodeling. Our current objective is 2-fold: (i) characterize the genomic responses to perceived hyperoxia in isolated cardiac fibroblasts using a DNA microarray approach and (ii) seek first *in vivo* evidence testing whether p21 expression is induced in the heart recovering from ischemia-reoxygenation.

MATERIALS AND METHODS

Cardiac Fibroblast Isolation and Culture

Experiments were performed using primary CF isolated from adult (5–6 weeks old) mouse ventricle using procedures described previously (6).

* The costs of publication of this article were defrayed in part by the payment of page charges. This article must therefore be hereby marked "*advertisement*" in accordance with 18 U.S.C. Section 1734 solely to indicate this fact.

[S] The on-line version of this article (available at http://www.jbc.org) contains Supplemental Figs. S1 and S2 and Table S1.

§ To whom correspondence should be addressed: 512 Davis Heart & Lung Research Inst., 473 W. 12th Ave., Columbus, OH 43210. Tel.: 614-247-7658; Fax: 614-247-7818; E-mail: sen-1@medctr.osu.edu.

[1] The abbreviations use are: CF, cardiac fibroblasts; MAS, Microarray Suite, version 5.0; DMT, Data Mining Tool, version 2.0; I-R, ischemia-reperfusion.

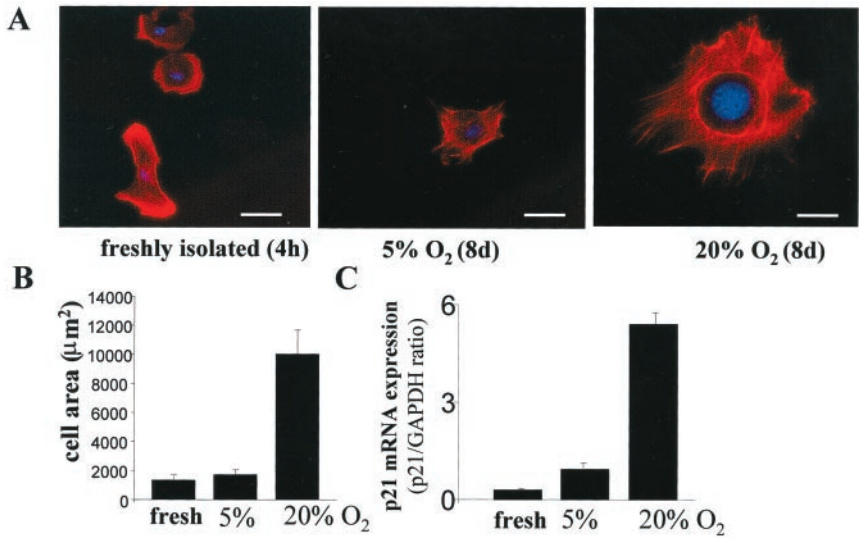

FIG. 1. **Freshly isolated CF are phenotypically closer to CF cultured at 5% O_2 compared with the CF cultured at higher O_2 tensions.** *A* and *B*, after isolation, CF were either (i) fixed 4 h after isolation or (ii) cultured at 5 or 20% O_2 for 8 days. *A*, for morphologic comparisons with freshly isolated CF fixed 4 h after isolation, CF cultured at various O_2 tensions for 8 days were trypsinized and reseeded. Cells were fixed 4 h after reseeding. The reseeding was performed to obtain comparable cell spreading in freshly isolated CF *versus* CF maintained in various O_2 environments for 8 days. Cells were stained with phalloidin (actin, *red*) and nuclei were stained with 4′,6-diamidino-2-phenylindole (*blue*). Imaging was performed using a Zeiss microscope. *Scale bar*, 20 μm. *B*, cell area quantification was performed using Axiovision software. *C*, quantification of p21 mRNA expression using real-time PCR. p21 data presented have been normalized for glyceraldehyde-3-phosphate dehydrogenase (*GAPDH*).

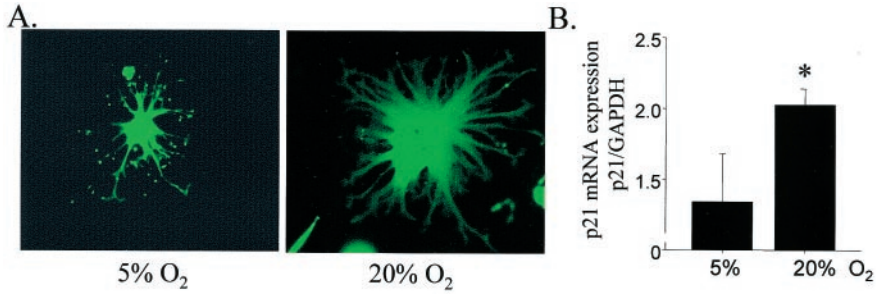

FIG. 2. **CF cultured in three-dimensional collagen matrices mimic the effect of oxygen observed in standard CF monolayer culture.** Three-dimensional culture of CF in collagen gel was performed as described under "Materials and Methods." *A*, after isolation CF were cultured in either 5 or 20% O_2 for 5 days. Cells were infected with adenoviral vectors carrying green fluorescent protein (Ad.GFP) gene followed by culturing the in three-dimensional collagen matrix. Images were collected 72 h after culture in three-dimensional collagen gels. *B*, for gene expression studies, cells were harvested from collagen gel after 72 h using collagenase digestion. RNA was extracted and p21 expression was determined using real-time PCR. *GAPDH*, glyceraldehyde-3-phosphate dehydrogenase.

GeneChip™ Probe Array Analysis

To identify sets of perceived hyperoxia sensitive genes in CF, we utilized the GeneChip™ approach (7, 8). CF were isolated and cultured in a moderately hypoxic condition at 3% O_2 (6). Five days after isolation, cells were split and exposed to either elevated (20% O_2; widely interpreted as *in vitro* normoxia) or the same (3%) O_2 tension for 20 h. Cells were harvested and the total RNA was extracted using the RNeasy kit (Qiagen). Targets were prepared for microarray hybridization according to previously described protocols (7, 8). To assess quality, the samples were hybridized for 16 h at 45 °C to GeneChip™ test arrays. Satisfactory samples were hybridized to the mouse genome arrays (U74Av2) for the screening of over 12,000 genes and expressed sequence tags. The arrays were washed, stained with streptavidin-phycoerythrin, and were then scanned with the GeneArray scanner (Agilent Technologies) in our own facilities. To allow for statistical treatment, data were collected from three experiments.

Data Analysis

Raw data were collected and analyzed using Affymetrix Microarray Suite, version 5.0 (MAS) and Data Mining Tool, version 2.0 (DMT) software. Additional processing of data was performed using dChip software (9). A detailed analysis scheme has been illustrated in Fig. 3. Statistical (*t* test) and comparison analysis were the two approaches utilized to identify differentially expressed genes (7). *t* test was performed using DMT on absolute files generated from MAS. Genes that significantly ($p < 0.05$) changed (increased or decreased) in the perceived hyperoxia (20% O_2) group compared with the 3% O_2 group were selected. Next, dChip (version 1.3, Harvard University) software was used to further filter genes using following criteria: (i) fold change >1.2; (ii) *t* test, $p < 0.05$; and (iii) present call in all experimental (20% O_2) samples for up-regulated genes and present call in all base-line (3% O_2) samples for down-regulated genes. Using comparison analysis in MAS, nine pairwise comparisons were generated from three experiments of both 3 and 20% O_2 groups. Average fold changes were calculated for both up- or down-regulated genes. Genes with 100% (9 out of 9 pairs) concordance in pairwise comparisons were selected. For data visualization, genes filtered using the statistical (*t* test) approach were subjected to hierarchical clustering using dChip (version 1.3) software. Functional categorization and pathway construction were performed using the following software/web resources: Gene Ontology Data Mining Tool (Affymetrix), KEGG (Kyoto Encyclopedia of Genes and Genomes), GenMAPP (10), DAVID (Data Base for Annotation, Visualization, and Integrated Discovery Verification) (11), and LocusLink (Swiss-Prot). Microarray data were verified using real-time PCR assay.

mRNA Quantitation

mRNA were quantified by real-time PCR assay using double-stranded DNA binding dye SYBR Green-I as described previously (6). The primer set used for individual genes are listed in Table S1 (see Supplemental Materials).

Immunofluorescence Microscopy

F-actin (phalloidin, dilution 1:40, Molecular Probes), α-smooth muscle actin (Sigma), and p21 (Santa Cruz Biotechnology) immunostaining

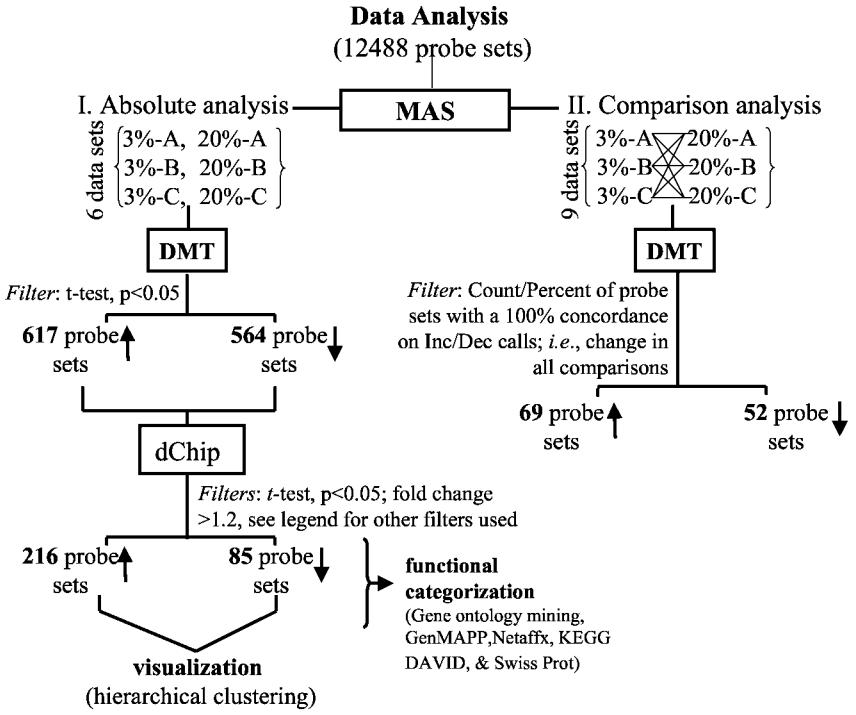

FIG. 3. **GeneChip™ data analysis scheme.** GeneChip™ data analysis scheme used to identify perceived hyperoxia-sensitive genes in three experiments (*A*, *B*, *C*) where cardiac fibroblasts were exposed to 3 or 20% O_2 for 20 h. Data processing was primarily performed using MAS and DMT software. Additional data filtration was performed using dChip using the following criteria: (i) fold change >1.2; (ii) *t* test, $p < 0.05$; and (iii) present call in all experimental (20% O_2) samples for up-regulated genes, vice versa present call in all base-line (3% O_2) samples for down-regulated genes. Details of software and other resources for data analysis have been provided under "Materials and Methods." ↑, increase; ↓, decreases in response to 20% O_2.

and microscopy (Zeiss Axiovert 200M) were performed as described previously (6).

Culture of CF in Three-dimensional Collagen Gels

Collagen lattices were prepared using type I collagen from rat tail tendon as described previously (12). CF were suspended in collagen (1.25 mg/ml) and aliquoted into culture plates. Collagen matrices were incubated in a cell culture incubator for 45 min followed by overlying the gel with Dulbecco's modified Eagle's medium containing 10% serum. Matrices were gently released after 24 h from the underlying culture dishes with a spatula and allowed to float in basal medium. Collagenase digestion was performed to harvest cells from collagen gel for gene expression studies.

Survival Model for Coronary Artery Occlusion and Reperfusion

Sprague-Dawley rats weighing 250–300 g were subjected to ischemia-reperfusion (I-R) of the heart. Parallel groups of rats were used as sham-operated controls. The studies were approved by the Animal Protection Committee of The Ohio State University. Rats were anesthetized, intubated, and mechanically ventilated on a positive pressure respirator with room air. The body temperature was maintained at 36–37 °C with a heated small animal operating table. A left thoracotomy was performed via the fifth intercostal space to expose the heart. A 30-min occlusion of left anterior descending coronary artery was followed by reperfusion. Laser Doppler flow measurement was used to verify I-R. Upon successful reperfusion, the thorax was closed, and negative thoracic pressure was re-established for survival. The rats were killed 2–7 days after reperfusion. For tissue harvesting, the infarcted I-R area was visualized under a dissecting microscope. Tissue samples were collected from infarcted (I-R) site as well as from a part of the left ventricle unaffected by I-R. As additional controls, tissues were collected from a location corresponding to the I-R and unaffected sites in sham-operated rats. These rats were exposed to all surgical procedures except I-R.

Histology

Histochemistry—Formalin-fixed tissues were embedded in paraffin and sectioned (4 μm) followed by hematoxilin and eosin staining.

Immunostaining—The sections were stained with the following primary antibodies: mouse monoclonal antibodies to p21 (1:50; Pharmingen) or anti-ED-1 (1:100; Serotec) and either horseradish peroxidase (p21) or fluorescent (ED-1)-tagged secondary antibodies. The ED-1-stained sections were counterstained with 4′,6-diamidino-2-phenylindole for nuclear staining.

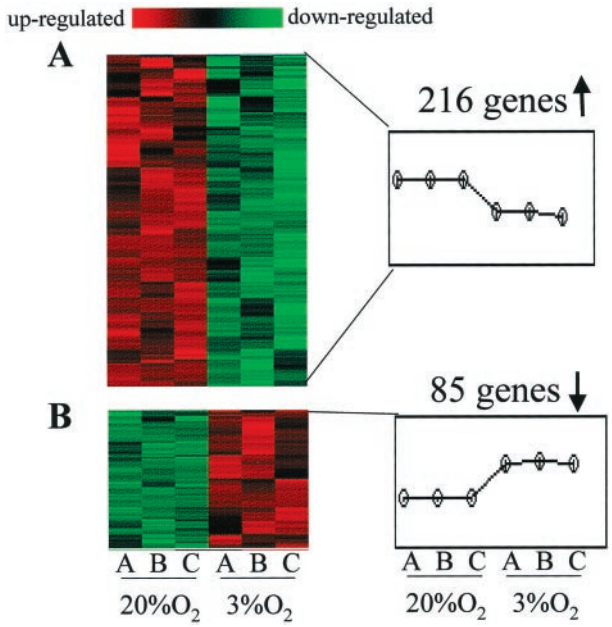

FIG. 4. **Cluster images illustrating genes sensitive to perceived hyperoxia.** For a clear graphic display of perceived hyperoxia-sensitive genes, the *t* test was performed on data from repeated experiments (*A*, *B*, *C*) involving 3 and 20% O_2 groups. The genes that significantly ($p < 0.05$) changed between the two groups compared were selected and subjected to hierarchial clustering using dChip software as described in the legend to Fig. 3. *Red* to *green* gradation in color represent higher to lower expression signal. *A* and *B*, up-regulated (*A*) or down-regulated (*B*) genes in 20% O_2 compared with 3% O_2 group.

In Vivo Hyperoxia Exposure

Male C57BL6 mice (5 weeks) were exposed to pure oxygen (hyperoxia) environment for 36 h. Control mice were maintained under similar conditions in room air (normoxia). p21 mRNA levels in myocardial tissue were evaluated by real-time PCR.

Statistics

The effect of perceived hyperoxia on p21 mRNA expression in hearts subjected to ischemia and reperfusion was analyzed using the Statistical Package for the Social Science, (Chicago, IL). Wilcoxon test was

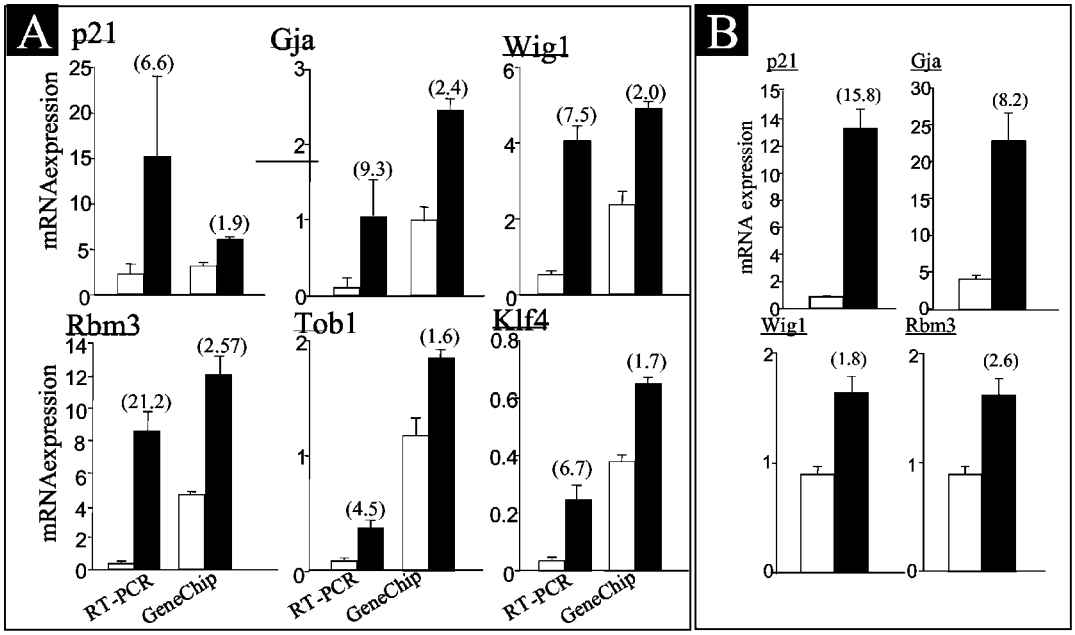

FIG. 5. **Real-time PCR validation of GeneChip™ microarray expression analysis.** Expression levels of selected genes identified using GeneChip™ analysis were independently determined using real-time PCR. For comparison, the GeneChip™ expression values were proportionately adjusted to fit to the scale with real-time PCR data. Fold change in 20% O_2 (*closed bars*) compared with 3% O_2 (*open bars*) group have been indicated in *parentheses*. *A*, RNA samples used in GeneChip™ assay were utilized for the real-time PCR analysis. The design includes isolation of CF followed by culturing then in 3% O_2 for 5 days. After 5 days cells are split and then exposed to either 3 or 20% O_2 for 20 h. *B*, After isolation CF were cultured in either 3 or 20% O_2 for 5 days. After splitting, 3 and 20% O_2 group were exposed to 3 and 20% O_2, respectively, for next 3 days. *p21*, cyclin-dependent kinase inhibitor 1A; *Gja*, gap junction membrane channel protein α 1; *Wig1*, wild-type p53-induced gene 1; *Rbm3*, RNA binding motif protein 3; *Tob1*, transducer of ErbB-2.1; *Klf4*, Krüppel-like factor 4. Fold changes are indicated in *parentheses*.

employed to compare the difference between pair-matched normal-perfused and I-R myocardial tissue. A p value < 0.05 was considered statistically significant. Statistics related to DNA microarray data processing are described above under "Data Analysis."

RESULTS

Under conditions of systemic normoxia, heart cells receive a limited supply of O_2 representing less than 10% (13–15). We have directly determined that mouse heart ventricular pO_2 is in the range of 5% (6). Thus, in this work 3, 5, and 20% O_2 are referred to as conditions representing mild hypoxia, normoxia, and perceived hyperoxia, respectively. Previously we have reported that the culture of isolated CF under room air (20% O_2) conditions results in major phenotypic changes including increased cell size and differentiation to myofibroblasts. In addition, perceived hyperoxia induced the expression of p21 (6). Our current results with isolated cardiac fibroblasts demonstrate that the phenotype of freshly isolated CF may be preserved under standard culture conditions by controlling the ambient O_2 condition to match the physiological pO_2 to which the cells are adjusted to *in vivo*. Maintenance of CF at 5% O_2 preserved cellular phenotype and did not result in the induction of the perceived hyperoxia-sensitive gene p21 (Fig. 1). Recently it has been identified that the study of fibroblasts in three-dimensional collagen matrices represents a powerful approach to model *in vivo* biology (12). Therefore, we sought to investigative whether the perceived hyperoxia induced phenotypic changes manifest during three-dimensional culture of CF. Indeed, both cell size as well as p21 expression was clearly increased in CF cultured in three-dimensional collagen matrices (Fig. 2). Under conditions of perceived hyperoxia, CF grown in collagen matrices exhibit increased contractile properties indicative of differentiation to myofibroblasts (6). Thus, our findings from our standard culture model are consistent with results obtained from three-dimensinal culture of CF.

In our previous study, we employed quantitative single-gene analysis approaches to determine that perceived hyperoxia influences genes related to cell cycle and differentiation (6). To obtain a comprehensive understanding of the genome-wide effects of perceived hyperoxia, we conducted a DNA microarray analysis of O_2-sensitive genes in CF. CF grown at 3 or 5% O_2 exhibits comparable phenotype and growth pattern. Thus, we sought to compare the transcriptome of CF grown at 3% O_2 with that of CF grown at 20% O_2. The objective was to identify sets of O_2-sensitive genes that would help us understand the biology of perceived hyperoxia. Three independent experiments were conducted so that appropriate data treatment could be possible. The data analysis design is illustrated in Fig. 3. Out of 12,488 probe sets screened, 5071 were present in CF at 3% O_2. Exposure of CF to 21% O_2 resulted in the detection of 5574 genes/expressed sequence tags as being present. Perceived hyperoxia resulted in the induction of 216 genes and down-regulation of 85 genes (Fig. 4). To obtain the biological significance of these findings, the genes sensitive to perceived hyperoxia were subjected to biological process categorization using Gene Ontology Data Mining (Affymetrix), GenMAPP, and DAVID. Fig. S1 illustrates the major functional categories identified using these approaches. Out of the 216 up-regulated probe sets uploaded, 109 had annotations for Gene Ontology biological process (Fig. S1*A*). For the 85 genes/expressed sequence tags down-regulated in response to perceived hyperoxia, 49 had annotations for Gene Ontology biological process (Fig. S1*B*). It was clear that among the annotated genes up-regulated in response to perceived hyperoxia, genes related to cell growth/maintenance and cell communications represent the largest functional categories. This finding is consistent with our previous results suggesting that perceived hyperoxia may play a key role in CF differentiation and tissue remodeling in the post-reoxygenation peri-infarct tissue. Next, genes sensitive to perceived hyperoxia were analyzed for cellular compartmentalization of their products using Gene Ontology Data Mining and DAVID. The major compartments affected are illustrated (Fig. S2). The total volume of up-regulated genes was roughly 2.5-

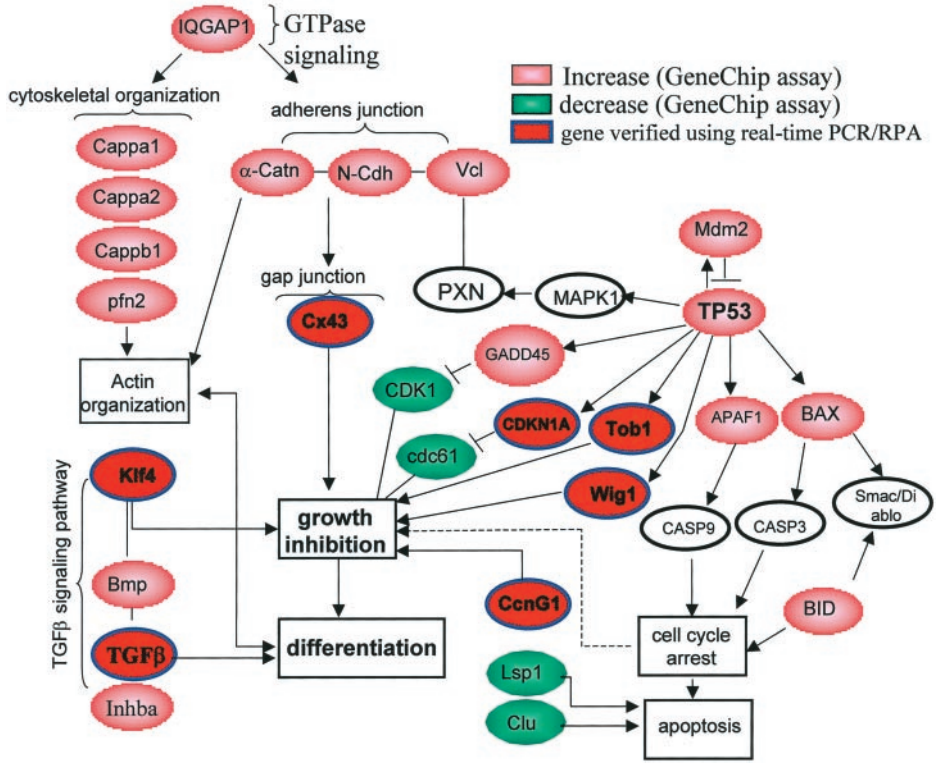

FIG. 6. **Pathway construction based on GeneChip™ expression data.** To obtain insights on perceived hyperoxia-induced changes in cell growth and differentiation on a pathway sense, the results of GeneChip™ analysis were mapped onto known pathways associated with cell cycle/death and cytoskeletal changes. GenMAPP, KEGG, and Gene Ontology were used to create the pathways. Genes shown in *red ellipse* are candidates identified using GeneChip™ assay that were up-regulated in 20% O_2 compared with 3% O_2. *Green ellipses* are genes that were down-regulated under conditions mentioned above. The expressions of candidates shown in *red ellipse* with *blue outline* have been independently verified using either real-time PCR or ribonuclease protection assay (6). *APAF*, apoptotic protease activating factor; *Bmp*, bone morphogenetic protein; *BAX*, Bcl2-associated X protein; *BID*, BH3 interacting domain death agonist; *Catn*, catenin; *Cappa*, capping protein α; *CASP*, caspage; *ccng*, cyclin G; *Cdc61*, cell division cycle; *CDK*, cyclin-dependent kinase; *CDKN1A*, cyclin-dependent kinase inhibitor 1A (p21); *Clu*, clusterin; *Cx43*, gap junction membrane channel protein; *GADD*, growth arrest and DNA damage-inducible; *IQGAP1*, IQ motif containing GTPase activating protein 1; *Inhba*, inhibin β-A; *Klf*, Krüppel-like factor 4 (gut); *Lsp1*, lymphocyte specific 1; *MAPK*, mitogen-activated protein kinase; *Mdm2*, transformed mouse 3T3 cell double minute 2; *N-Cdh*, cadherin 2; *Pfn*, profilin 2; *PXN*, paxillin; *TGF*, transforming growth factor; *Tob*, transducer of ErbB-2.1; *TP53*, transformation-related protein 53; *Vcl*, vinculin; *Wig*, wild-type p53-induced gene 1.

fold higher than the down-regulated genes. Growth arrest and differentiation are largely driven by nuclear gene products. Consistently, genes with products associated with nuclear function were observed to be a large group sensitive to perceived hyperoxia. Of interest, genes encoding cytoskeletal proteins were specifically induced in response to perceived hyperoxia (Fig. S2). This finding is consistent with our claim that perceived hyperoxia potently influences cellular phenotype.

To validate our DNA microarray results, the expression of select perceived hyperoxia sensitive genes were independently determined using real-time PCR. Using this approach, we typically find that the microarray approach underestimates the magnitude of change while reliably detecting the direction of change (Fig. 5*A*). To test the robustness of the findings, we conducted independent experiments with a more long-term O_2 exposure design (Fig. 5*B*). These efforts led to successful verification of findings obtained from the experiments conducted for the microarray study (Fig. 5*A*). To obtain an understanding of how the perceived hyperoxia-sensitive genes are related with respect to signaling pathways, the candidate genes were mapped onto known pathways associated with cell cycle/death and cytoskeletal changes. GenMAPP, KEGG, and Gene Ontology tools were used to reconstruct the pathways. The relevant signaling pathways that were derived using this approach identified growth inhibition and fibroblast differentiation as two related outcomes that are induced by perceived hyperoxia (Fig. 6).

To document the incidence of perceived hyperoxia *in vivo*, we developed a survival surgery model involving ischemia-reoxygenation of the rat heart. The objective was to examine the post-reoxygenation tissue for the induction of p21, a key perceived hyperoxia-sensitive gene (6). The affected site was histologically characterized for reoxygenation injury and inflammation (Fig. 7). Staining of the affected site revealed increased presence of p21 in post-reoxygenation tissue (Fig. 8*A*). This finding was verified by real-time PCR (Fig. 8*B*). To obtain proof of principle that p21 expression in the heart is indeed sensitive to hyperoxia *in vivo*, male C57BL6 mice were exposed to a pure oxygen environment for 36 h. Control mice were maintained under similar conditions in room air. Evaluation of mRNA levels in myocardial tissue using real-time PCR showed multifold increase in the expression of p21 following hyperoxic insult (Fig. 8).

DISCUSSION

Cardiac remodeling leads to changes in the extracellular matrix, and in some cases to cardiac fibrosis, a process involving myofibroblasts as an active component. Myofibroblasts are phenotypically distinct. They are larger and more stellate, proliferate slowly, and have the most prominent microfilament arrays. We have recently proposed that reoxygenation of an ischemic site, in addition to being a trigger for injury, may induce tissue remodeling. We observed that exposure to a higher pO_2, relative to which cells are adjusted, induces the differentiation of CF to myofibroblasts. This is of significant relevance to cardiac tissue remodeling in the face of reoxygen-

ation (6). In the absence of robust *in vivo* models for chronic low flow we have turned toward the study of isolated CF, key players in tissue remodeling. The culture of isolated CF under conditions of O_2-rich room air results in a clear switch of phenotype compared with the phenotype of freshly isolated CF. In this work we report direct evidence demonstrating that solely by maintaining the O_2 ambience of the culture condition to a level closely matching *in vivo* ventricular pO_2, such culture-dependent switch of phenotype may be prevented. These findings further support the contention that changes in O_2 environment is a cue that CF sensitively responds to. Fibroblast biology in three-dimensional collagen matrices closely models *in vivo* situations (12). Under such conditions, cells exhibit a distinct phenotype referred to as dendritic fibroblasts (12). Our observation that perceived hyperoxia induces the expression of p21, increase in cell size, and differentiation to myofibroblast (6) has been confirmed in CF grown in a three-dimensional matrix. Indeed, myofibroblasts have been detected abundantly in healing myocardial reperfused infarcts (16).

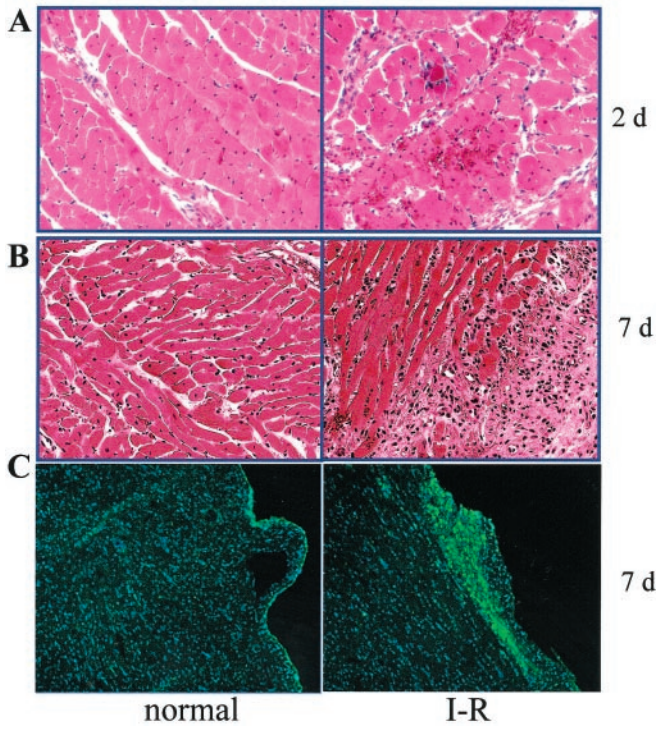

FIG. 7. **Histologic evaluation of myocardium following ischemia-reperfusion.** Occlusion (30 min) of left anterior descending coronary artery was followed by reperfusion for 2 or 7 days. Tissue samples were collected from infarcted (*I-R*) or normally (*normal*) perfused ventricular myocardium. *A* and *B*, hematoxylin and eosin staining of the myocardium. Note the infiltration of inflammatory cells and damaged myocardium. *C*, presence of macrophages (*green*, ED-1 antibody staining) at the I-R site.

Application of the high density DNA microarray approach coupled with current bioinformatics tools enabled us to identify sets of O_2-sensitive genes in CF and categorize them into functional groups. In addition, the candidate genes have been categorized with respect to the cellular localization of their products. That low O_2 ambience serves as a cue to trigger angiogenesis is a well accepted notion. We have previously demonstrated that the sensing of O_2 environment is not limited to hypoxia but extends to perceived hyperoxia as well (6). Our current report constitutes first evidence demonstrating that the culture of cells, isolated from an organ, at room air condition results in specific and significant genome-wide changes. As we strive to improve *in vitro* approaches to study cell biology relevant to *in vivo* conditions, a careful consideration of the O_2-ambience is clearly warranted. Furthermore, the results provide a comprehensive definition to perceived hyperoxia establishing that cell communication and cell growth/maintenance are indeed the primary outcomes affected. Both of these processes are tightly linked to cellular differentiation and tissue remodeling (6, 17). Recently it has been proposed that

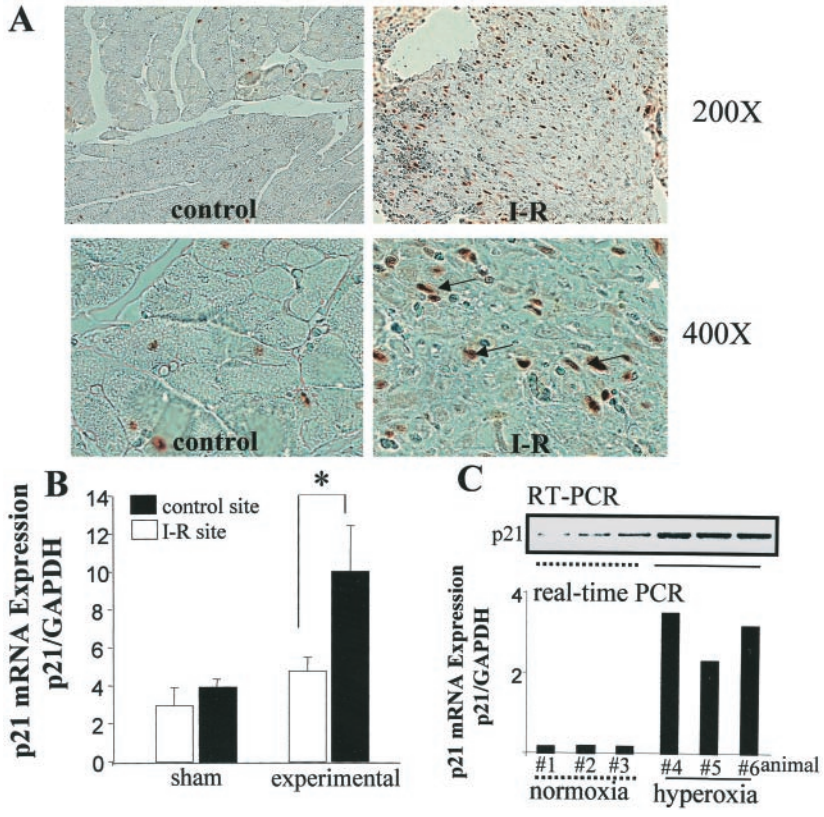

FIG. 8. **Activation of p21 in myocardial tissue following ischemia/reperfusion and hyperoxic insult.** *A* and *B*, occlusion (30 min) of left anterior descending coronary artery was followed by reperfusion for 7 days. Tissue samples were collected from infarcted (*I-R*) or normally (*control*) perfused ventricular myocardium. Samples from control and I-R sites were also collected from sham-operated animals as additional control samples. *A*, immunolocalization of p21 protein (*brown*) in myocardium following ischemia (30 min) and reperfusion (7 days). *Upper panel*, ×200 magnification; *lower panel*, ×400 magnification. *B*, quantification of p21 mRNA expression using real-time PCR; paired data (mean ± S.E.; $n = 14$) shown from animals underwent ischemia (30 min) and reperfusion (7 days). *, $p < 0.05$ significantly different compared with its pair-matched normal-perfused tissue. *C*, male C57BL6 mice were exposed to 100% oxygen (*hyperoxia*) environment for 36 h. Control mice were maintained in room air (*normoxia*). p21 mRNA levels in myocardial tissue were evaluated by real-time PCR. Data for individual animals have been presented to demonstrate tight uniformity of the findings. *GAPDH*, glyceraldehyde-3-phosphate dehydrogenase.

many of the signaling pathways that control cellular decisions related to tissue remodeling are regulated by nuclear interactions of cell cycle proteins (18). Indeed, our results demonstrate that nuclear proteins represent one of the largest categories of products encoded by genes sensitive to perceived hyperoxia. Using the perceived hyperoxia-sensitive gene sets that we have identified previously (6), and the sets identified in the current study, our pathway reconstruction results characterize the specific effects of perceived hyperoxia on cell cycle.

Select candidate genes that have been verified using quantitative real-time PCR include p21 (6), Wig-1, Gja, Rbm3, Tob1, and Klf4. The transcription factor Krüppel-like factor 4 (Klf4) supports p53-dependent cell cycle arrest (19) and differentiation (20). Tob is a member of the p53-independent, as well as -dependent, anti-proliferative family genes (21, 22). A critical role of Tob in checking cell cycle is suggested by findings that mice lacking Tob are predisposed to a higher incidence of cancer (23). The nuclear glycine-rich ribonucleoprotein RNA binding motif protein 3 (Rbm3) (24) has translation regulatory functions, the cardiovascular significance of which remains to be characterized. Gap junctions are widely distributed structures that mediate communication between cells. The channels that allow passage of small molecules between adjacent cells are made up of connexins that are encoded by a family of related genes. In the heart, connexins ensure electric and metabolic coupling between cells. Cell-cell communication is a key process during differentiation and typically it is down-regulated during cell proliferation. Gap junction gene A1 (*Gja1*) or connexin 43 is essentially required for coronary artery development and patterning (25). Thus, a central remodeling role of this gene in the healing tissue is expected. In humans, defect in connexin 43 result in visceroatrial heterotaxia (26). Wig-1 represents a stress-responsive p53-induced growth-inhibitory zinc finger protein (27). It is nuclear localized and binds to double-stranded RNA (28). Double-stranded RNA binding proteins are emerging as evolutionarily conserved key regulatory mechanisms modulating fine aspects of gene expression including translation, RNA editing, and stability (29).

p21 supports remodeling of tissues injured by oxygenation (30). Our previous work identified p21 as a key mediator of the effects of perceived hyperoxia (6). Here we present first evidence demonstrating the induction of p21 in post-reoxygenated recovering myocardial tissue. Other responses to perceived hyperoxia include transforming growth factor-β activation and differentiation of fibroblasts to myofibroblasts (6). Both of these have been identified in the myocardial tissue recovering from reoxygenation injury (16, 31). More recent studies present transforming growth factor-β as an important mediator of post-reperfusion healing (32), consistent with our proposed role of perceived hyperoxia in facilitating tissue remodeling. That low oxygen ambience serves as a cue to trigger angiogenesis is a well accepted notion. Our studies establish that the sensing of oxygen environment is not limited to hypoxia. Our studies demonstrate that in addition to being a trigger for injury as is widely recognized, reoxygenation insult has a built-in component of tissue remodeling induced by perceived hyperoxia. It is plausible that in the event of minor injuries that go unnoted in our daily lives, such remodeling serves to heal as a physiological reparative mechanism. Understanding of this physiological healing response may offer novel opportunities to manage more intense reoxygenation injuries.

REFERENCES

1. Semenza, G. L. (2001) *Cell* **107,** 1–3
2. Porwol, T., Ehleben, W., Brand, V., and Acker, H. (2001) *Respir. Physiol.* **128,** 331–348
3. Rumsey, W. L., Pawlowski, M., Lejavardi, N., and Wilson, D. F. (1994) *Am. J. Physiology.* **266,** H1676–H1680
4. Siaghy, E. M., Devaux, Y., Sfaksi, N., Carteaux, J. P., Ungureanu-Longrois, D., Zannad, F., Villemot, J. P., Burlet, C., and Mertes, P. M. (2000) *J. Mol. Cell. Cardiol.* **32,** 493–504
5. Eghbali, M., Czaja, M. J., Zeydel, M., Weiner, F. R., Zern, M. A., Seifter, S., and Blumenfeld, O. O. (1988) *J. Mol. Cell. Cardiol.* **20,** 267–276
6. Roy, S., Khanna, S., Bickerstaff, A. A., Subramanian, S. V., Atalay, M., Bierl, M., Pendyala, S., Levy, D., Sharma, N., Venojarvi, M., Strauch, A., Orosz, C. G., and Sen, C. K. (2003) *Circ. Res.* **92,** 264–271
7. Roy, S., Khanna, S., Bentley, K., Beffrey, P., and Sen, C. K. (2002) *Methods Enzymol.* **353,** 487–497
8. Roy, S., Lado, B. H., Khanna, S., and Sen, C. K. (2002) *FEBS Lett.* **530,** 17–23
9. Li, C., and Wong, W. H. (2001) *Proc. Natl. Acad. Sci. U. S. A.* **98,** 31–36
10. Dahlquist, K. D., Salomonis, N., Vranizan, K., Lawlor, S. C., and Conklin, B. R. (2002) *Nat. Genet.* **31,** 19–20
11. Dennis, G., Jr., Sherman, B. T., Hosack, D. A., Yang, J., Gao, W., Lane, H. C., and Lempicki, R. A. (2003) *Genome Biology* http://genomebiology.com/2003/4/5/P3
12. Grinnell, F., Ho, C. H., Tamariz, E., Lee, D. J., and Skuta, G. (2003) *Mol. Biol. Cell* **14,** 384–395
13. Winegrad, S., Henrion, D., Rappaport, L., and Samuel, J. L. (1999) *Circ. Res.* **85,** 690–698
14. Gonschior, P., Gonschior, G. M., Conzen, P. F., Hobbhahn, J., Goetz, A. E., Peter, K., and Brendel, W. (1992) *Basic Res. Cardiol.* **87,** 27–37
15. Whalen, W. J. (1971) *Physiologist* **14,** 69–82
16. Frangogiannis, N. G., Michael, L. H., and Entman, M. L. (2000) *Cardiovasc. Res.* **48,** 89–100
17. Scott, J. D., and Pawson, T. (2000) *Sci. Am.* **282,** 72–79
18. Nabel, E. G. (2002) *Nat. Rev. Drug Discov.* **1,** 587–598
19. Yoon, H. S., Chen, X., and Yang, V. W. (2003) *J. Biol. Chem.* **278,** 2101–2105
20. Jaubert, J., Cheng, J., and Segre, J. A. (2003) *Development* (*Camb.*) **130,** 2767–2777
21. Tirone, F. (2001) *J. Cell. Physiol.* **187,** 155–165
22. Kuo, M. L., Duncavage, E. J., Mathew, R., den Besten, W., Pei, D., Naeve, D., Yamamoto, T., Cheng, C., Sherr, C. J., and Roussel, M. F. (2003) *Cancer Res.* **63,** 1046–1053
23. Yoshida, Y., Nakamura, T., Komoda, M., Satoh, H., Suzuki, T., Tsuzuku, J. K., Miyasaka, T., Yoshida, E. H., Umemori, H., Kunisaki, R. K., Tani, K., Ishii, S., Mori, S., Suganuma, M., Noda, T., and Yamamoto, T. (2003) *Genes Dev.* **17,** 1201–1206
24. Derry, J. M., Kerns, J. A., and Francke, U. (1995) *Hum. Mol. Genet.* **4,** 2307–2311
25. Li, W. E., Waldo, K., Linask, K. L., Chen, T., Wessels, A., Parmacek, M. S., Kirby, M. L., and Lo, C. W. (2002) *Development* (*Camb.*) **129,** 2031–2042
26. Britz-Cunningham, S. H., Shah, M. M., Zuppan, C. W., and Fletcher, W. H. (1995) *N. Engl. J. Med.* **332,** 1323–1329
27. Hellborg, F., Qian, W., Mendez-Vidal, C., Asker, C., Kost-Alimova, M., Wilhelm, M., Imreh, S., and Wiman, K. G. (2001) *Oncogene* **20,** 5466–5474
28. Mendez-Vidal, C., Wilhelm, M. T., Hellborg, F., Qian, W., and Wiman, K. G. (2002) *Nucleic Acids Res.* **30,** 1991–1996
29. Saunders, L. R., and Barber, G. N. (2003) *FASEB J.* **17,** 961–983
30. Staversky, R. J., Watkins, R. H., Wright, T. W., Hernady, E., LoMonaco, M. B., D'Angio, C. T., Williams, J. P., Maniscalco, W. M., and O'Reilly, M. A. (2002) *Am. J. Pathol.* **161,** 1383–1393
31. Herskowitz, A., Choi, S., Ansari, A. A., and Wesselingh, S. (1995) *Am. J. Pathol.* **146,** 419–428
32. Chen, H., Li, D., Saldeen, T., and Mehta, J. L. (2003) *Am. J. Physiol.* **284,** H1612–H1617

Characterization of Perceived Hyperoxia in Isolated Primary Cardiac Fibroblasts and in the Reoxygenated Heart

Sashwati Roy, Savita Khanna, William A. Wallace, Jani Lappalainen, Cameron Rink, Arturo J. Cardounel, Jay L. Zweier and Chandan K. Sen

J. Biol. Chem. 2003, 278:47129-47135.
doi: 10.1074/jbc.M308703200 originally published online September 2, 2003
